Main properties of Al_2O_3 thin films deposited by magnetron sputtering of an Al_2O_3 ceramic target at different radio-frequency power and argon pressure and their passivation effect on *p*-type *c*-Si wafers

J.A. García-Valenzuela[a]*, R. Rivera[a,†], A.B. Morales-Vilches[b,‡], L.G. Gerling[b], Á. Caballero[a],
J.M. Asensi[a], C. Voz[b], J. Bertomeu[a], J. Andreu[a]

[a] *Departament de Física Aplicada (FA), Universitat de Barcelona (UB), Carrer de Martí i Franquès 1–11, C.P. 08028, Barcelona, Catalonia, Spain.*
[b] *Departament d'Enginyeria Electrònica (DEE), Universitat Politècnica de Catalunya (UPC), Carrer de Jordi Girona 1–3, C.P. 08034, Barcelona, Catalonia, Spain.*

* Corresponding author. Tel.: +34 934 039221; fax: +34 934 039218.
E-mail addresses: jgarciavlz@ub.edu, jgarciavlz@gmail.com (J.A. García-Valenzuela).

[†] Present address: *Sección de Fisicoquímica, Departamento de Química, Universidad Técnica Particular de Loja (UTPL), Calle Marcelino Champagnat S/N, A.P. 11-01-608, Loja, Loja, Ecuador.*

[‡] Present address: *Kompetenzzentrum Dünnschicht- und Nanotechnologie für Photovoltaik Berlin (PVcomB), Helmholtz-Zentrum Berlin für Materialen und Energie (HZB) GmbH, Schwarzschildstraße 3, D-12489, Berlin-Adlershof, Germany.*

Abstract

In this work, 50-nm thick Al_2O_3 thin films were deposited at room temperature by magnetron sputtering from an Al_2O_3 ceramic target at different RF power and argon pressure values. The sputtering technique could be preferred to conventional atomic layer deposition for an industrial application, owing to its simplicity, availability, and higher deposition rate. The resulting thin films were characterized by UV/Vis/NIR spectroscopy, X-ray diffraction, and X-ray photoelectron spectroscopy. The deposited Al_2O_3 material was always highly transparent and amorphous in nature. It was found that the O/Al ratio is higher when the Al_2O_3 layer is deposited at lower RF power or higher argon pressure. Also, some argon incorporation into the films was observed at low deposition pressure. On the other hand, the performance of the previously characterized Al_2O_3 thin films in the passivation of 2.25-Ωcm *p*-type float zone *c*-Si wafer surfaces was evaluated by the quasi-steady-state photoconductance technique. The best effective carrier lifetime value at one-sun illumination, 0.34 ms (corresponding to a surface recombination velocity of 41 cm/s), was obtained with the 50-nm Al_2O_3 deposited at the higher argon pressure studied, 0.67 Pa (5.0 mTorr), with the lowest RF power studied, 150 W (corresponding to a power density of 3.3 W/cm^2), and after an annealing process, in this case at 350 ºC for 20 min with forming gas. It was assumed that the reduction of the surface passivation quality at higher RF power or lower argon pressure is a consequence of an increased surface damage, and, probably, to a decrease of the O/Al ratio of the Al_2O_3 passivation material. These assumptions were confirmed with the obtainment of a lifetime of 0.73 ms (a surface recombination velocity equal to 19 cm/s) with a simple experiment with Al_2O_3 deposited with progressively varied sputtering conditions started from minimal silicon surface damage conditions: 50 W (corresponding to a power density of 1.1 W/cm^2) and 6.67 Pa (50 mTorr). Finally, comments about further improvement of the effective lifetime (up to 1.25 ms, corresponding to a surface recombination velocity of 11 cm/s) with preliminary experiments about the incorporation of an intrinsic hydrogenated amorphous silicon interlayer are included.

Keywords: Alumina; Sputtering; RF power; Silicon; Surface passivation; Quasi-steady-state photoconductance; Lifetime.

1. Introduction

Nowadays, crystalline silicon (*c*-Si) and polycrystalline silicon (poly-Si) wafers constitute most of the solar cell technology, having the highest market share. The efficiency of *c*-Si solar cells is, however, reduced by recombination of photogenerated carriers at the silicon wafer surfaces. This aspect is gaining relevance, as thinner wafers (<200 μm) are progressively introduced in production lines. Therefore, the reduction of this surface recombination, called surface passivation, is very important in the performance of low-cost and high-efficiency *c*-Si solar cells.

It is known that the surface passivation can be achieved by means of two different strategies [1–7]. The first of them, called chemical passivation, refers to the reduction of interface state density (D_{it}) at the silicon surface, which can be achieved, for example, through the passivation of silicon dangling bonds by hydrogen atoms. The second one, called field-effect passivation, which consists of producing a band bending at the silicon surface, refers to the reduction in the density of one type of minority charge carrier present at the silicon surface by an electric field; this can be obtained, for example, by fixed charge (Q_{f}) present in the thin film deposited on the silicon surface.

Among the common passivation materials, the Al_2O_3 one is currently gaining relevance [1–11], since the passivation by Al_2O_3 thin films, particularly by Al_2O_3 deposited by the atomic layer deposition (ALD) technique, is typically a combination of both chemical and field-effect passivation mechanisms [2,3]. This material contains a very high density of negative charges—high Q_{f}—and, as an inherent effect of the ALD technique, the deposited material acts as a hydrogen reservoir providing hydrogen atoms to the $Si/SiO_x/Al_2O_3$ interface formed or restructured during thermal treatments, thus reducing D_{it}. (This interest in ALD-deposited Al_2O_3 originated with works of Agostinelli *et al.* [12] and Hoex *et al.* [13], both reported in 2006.)

Although ALD-deposited Al_2O_3 shows the better passivation results, the ALD technique is not currently appropriate for large-scale production because of a limited throughput. The deposition rate of Al_2O_3 by conventional ALD equipments is typically below than 0.5 nm/min. However, the high-rate spatial ALD can overcome this limitation, but at the expense of higher system cost and complexity [14]. Nevertheless, the current industry of metal oxide film deposition is dominated by other techniques, such as magnetron sputtering. However, this industrially suitable technique, in comparison to the ALD one, has not been extensively studied in relation to the *c*-Si passivation by Al_2O_3, maybe due to the relatively lower surface passivation quality usually obtained [8–10].

In the previous context, Cuevas and collaborators took the challenge of improving the passivation of *c*-Si by means of Al_2O_3 deposited by sputtering, and demonstrated in a sequence of papers [15–20] that such a material deposited by radio-frequency (RF) sputtering is suitable of providing good silicon surface passivation. However, a complete correlation between deposition conditions and the resulted passivation is lacking to date. Furthermore, the experiments by the group of Cuevas were developed exclusively with reactive sputtering of an Al metallic target, which increases the deposition parameters to be controlled.

Therefore, in this paper we present a study of the main characteristics of Al_2O_3 thin films deposited by RF sputtering of an Al_2O_3 ceramic target under different RF power and deposition pressure values, and the passivation of *c*-Si wafers obtained by the effect of these Al_2O_3 films deposited under the studied sputtering conditions. Specifically, we are focused on the overall effect of the mentioned sputtering parameters on the passivation of *p*-type *c*-Si by the deposited Al_2O_3, and, where possible, in the correlation of the Al_2O_3 characteristics with the passivation results of *p*-type *c*-Si wafers, according to the studied sputtering conditions. It is expected that the results lead to a better understanding of the passivation of *c*-Si wafers due to the sputtering-deposited Al_2O_3, and thus allows to design a scheme to improving the passivation results by this industrially relevant deposition technique.

2. Experimental details

The experimental design for developing this work is divided into two subsections: 1) the deposition and routine characterization of the Al_2O_3 thin films deposited on glass substrates, and 2) the passivation effect of such Al_2O_3 thin films deposited on the *p*-type *c*-Si wafer surfaces, assessed from the measurements of carrier lifetimes.

2.1. Deposition and characterization of Al_2O_3 on glass substrates

The deposition equipment used in the present work was a commercial ATC-ORION 8 HV sputtering system from AJA International, Inc. It consisted of a 34.7-cm diameter and 39.8-cm height chamber with 3 different magnetron guns in a con-focal geometry. In this configuration, the magnetron sputter guns, which can host targets of 7.62 cm (3 inch) in diameter, are 3° tilted and located 10 cm off-axis of the substrate. The Al_2O_3 thin films were deposited at room temperature onto 5×5 cm^2 1737F Corning glass substrates by RF magnetron sputtering from a 99.99% purity Al_2O_3 ceramic target. Before each deposition process, the glass substrate to be used was washed with deionized water and liquid soap, then it was rinsed first with abundant deionized water and later with abundant isopropanol, and finally it was dried with nitrogen gas and placed on the holder-plate inside the sputtering chamber.

The distance from the center of the target to the center of the substrate was fixed at 18 cm, and a substrate rotation of 13 rpm was used to achieve a good homogeneity during the material deposition. The base pressure achieved before deposition was always between 2.7×10^{-4} Pa (2×10^{-6} Torr) and

4.0×10^{-4} Pa (3×10^{-6} Torr), which were measured with a Granville-Phillips 274 Bayard-Alpert type ionization vacuum gauge. The working gas was 99.99% argon. In this work, we studied the effect of RF power and deposition pressure (exclusively argon gas) on the characteristics and properties of Al_2O_3 thin films deposited on glass substrates. For this, the RF power values of 150, 300, and 450 W were studied; these values correspond, when divided by the target area (45.60 cm^2), to the power densities of 3.3, 6.6, and 9.9 W/cm^2, respectively. On the other hand, the studied deposition pressure values were 0.13 Pa (1.0 mTorr), 0.33 Pa (2.5 mTorr), and 0.67 Pa (5.0 mTorr); these pressure values were manually adjusted while maintaining constant the argon flow with a value of 20 sccm.

A Dektak 3030 mechanical surface profiler, which is equipped with a 25 μm diameter probe, has been used to determine the thickness of the samples. In the deposited film, some steps were created by means of a simple lift-off technique. Thus, the depth of the steps could be precisely measured with the profiler, which has a vertical resolution of 1 nm. The obtained results were corroborated by confocal microscopy thanks to a Sensofar PLμ 2300 optical imaging profiler device. A first set of deposited films was measured to calculate the deposition rate under the two studied parameters, by assuming a constant deposition rate along the film growing process, and the results are plotted in **Figure 1**. The resulting values were used to calculate the deposition time required to obtain 50-nm thick thin films, which is a common value used to passivate silicon wafers. This thickness of 50 nm was also corroborated in all the samples by means of the Sensofar PLμ 2300 optical imaging profiler device.

The percent transmittance ($\%T$) and percent reflectance ($\%R$) of the glass substrate covered with the deposited 50-nm Al_2O_3 thin films were measured by using a PerkinElmer Lambda 950 UV/Vis/NIR spectrometer in the 250 to 2500 nm wavelength interval. The $\%T$ was also integrated in the interval of 400 to 1100 nm in all the cases. The measurements were carried out with the Al_2O_3 thin films facing the incident light.

With the aim of finding some degree of crystallinity in the deposited Al_2O_3 material, the films were also analyzed by X-ray diffraction (XRD) by using a PANalytical X'Pert PRO MPD Alpha 1 powder X-ray diffractometer. Finally, the chemical bonding of the Al_2O_3 material was analyzed through X-ray photoelectron spectroscopy (XPS) by using a PHI 5500 Multitechnique system (from Physical Electronics), with a monochromatic X-ray source from Al Kα line with an energy of 1,486.8 eV. The measured binding energies were charge-corrected by referencing the C 1*s* peak to 284.80 eV, which is usually assigned to the adventitious hydrocarbon [21a].

2.2. Al_2O_3 passivation effect on p-type c-Si wafers

In order to create a symmetrical structure, the Al_2O_3 thin films were deposited onto both sides of *p*-type *c*-Si wafers (high-quality float zone silicon wafers, 10 cm in diameter, 280 μm in thickness, and resistivity of 2.25 Ωcm). The deposition conditions were the same as previously described for glass substrates. Before deposition, a careful cleaning process of the silicon wafer surface is crucial to obtain high passivation values. The importance of this step lies on the fact that possible impurities remaining on the wafer surface would act as recombination centers. In this work, the samples were initially cleaned using a two-steps standard wafer cleaning sequence known as RCA standard clean process [22–24a]. The first step of the process removes the organic surface contamination by means of an alkaline etching (RCA standard clean 1, RCA 1) with H_2O:H_2O_2:NH_3 (6:1:1 for our case) for 20 minutes at 70 ºC. The second step removes the possible metal contamination of the surfaces with an acid etching (RCA standard clean 2, RCA 2) employing H_2O:H_2O_2:HCl (6:1:1 for our case) for 10 minutes at 70 ºC. Between RCA 1 and RCA 2 it is necessary a 60-s etching time in 1% hydrofluoric acid (HF) in order to remove the SiO_2 grown in the surface during the RCA 1. Finally, after the RCA 2 it is necessary another 60 s of immersion in 1% HF to remove the SiO_2 grown in the second RCA step. The depositions of Al_2O_3 were done immediately after finishing this last acid cleaning.

The performance of the sputtering-deposited Al_2O_3 as a passivation layer for *p*-Si wafers was evaluated from the effective lifetime of photogenerated carriers, which was measured by the quasi-steady-state photoconductance (QSSPC) technique with a WCT-120 Silicon Wafer Lifetime Tester, from Sinton Consulting Inc. The effective lifetime (τ_{eff}) of the minority carriers measured by the instrument can be related to recombination processes in the bulk and at the surfaces through the following equation [24b,25]:

$$\frac{1}{\tau_{\mathrm{eff}}} = \frac{1}{\tau_{\mathrm{bulk}}} + \frac{2S_{\mathrm{eff}}}{W} \quad , \qquad (1)$$

where τ_{bulk} is the lifetime in the bulk (with a value higher than 4 ms, as certified by the supplier for the *p*-Si wafers used in the present work), W is the wafer thickness (0.028 cm for the present case), and S_{eff} is the effective surface recombination velocity, that can be assumed equal on both sides of the symmetrical structure. For the high quality wafers used in this study (very long τ_{bulk}), the τ_{eff} is mainly limited by surface recombination, and the S_{eff} value can be obtained from:

$$S_{\mathrm{eff}} \leq \frac{W}{2\tau_{\mathrm{eff}}} \quad . \qquad (2)$$

Both measured τ_{eff} and calculated S_{eff} values were used to assess the passivation of the *p*-type *c*-Si wafers by sputtering-deposited Al_2O_3 thin films.

3. Results and discussion

The following text is divided into three subsections: the first one for the main characteristics and properties of the Al_2O_3 layers deposited by sputtering on glass substrates and the second subsection for the surface passivation of the *p*-type *c*-Si wafers with Al_2O_3; a third subsection is included for additional comments and future works.

3.1. Characteristics and properties of the sputtering-deposited Al_2O_3 thin films

As shown in **Figure 1** (which was previously mentioned), it is observed that the deposition rate increases with the applied power, which is due to the higher energy introduced to the particles. On the other hand, the deposition rate decreases as the deposition pressure increases, due to the reduction of the mean free path when higher pressures are used, which increases the number of particles in the plasma and therefore the probability of collisions. It is observed also that while the effect of RF power was very significant on the deposition rate, the effect of deposition pressure was slight. Therefore, in the studied cases, the deposition rate is governed mainly by the deposition power.

At first sight, all the deposited Al_2O_3 thin films were completely transparent, with an appearance very similar to the glass substrate. It was observed through optical measurements that all the 50-nm Al_2O_3 thin films show very similar *%T* and *%R* values, independently of the RF power or deposition pressure. Some results of these measurements are presented in **Figure 2** and **Figure 3**, where, for the first case, the RF power was constant at 300 W and the deposition pressure was varied, and, for the second case, the deposition pressure was maintained constant at 0.67 Pa (5.0 mTorr) while the RF power was varied. In order to quantify the slight change in the *%T*, which seems to be mainly due to the increase in *%R*, as observed in the spectra, the measured values for *%T* were integrated in the interval of 400 to 1100 nm (which is the interval of interest for *c*-Si solar cells) and the results are presented in **Table 1**. The calculated values are around 91.5%, compared with the 94.1% corresponding to the uncovered glass substrate. These results confirm that the deposited Al_2O_3 material is very transparent, allowing the pass of the incident light to the substrate. As an additional comment, it is observed a slight increase in the calculated integrated *%T* when both the RF power and deposition pressure are increased, but the difference is not greater than ~0.8%.

All the deposited thin films were studied by means of XRD in order to determine any possible degree of crystallinity. **Figure 4** shows the diffractograms for the Al_2O_3 thin films deposited at 0.67 Pa (5.0 mTorr) and different RF powers, as examples. As it can be seen, it was not possible to detect any defined peak in the diffractograms, which implies that no crystallinity degree is found in the deposited 50-nm Al_2O_3. This amorphous nature was found in all the deposited films, regardless of the RF power or deposition pressure. On the other hand, in an attempt to determine whether this amorphous state could be attributed to the initial nucleation, which is dominant in very thin films, another Al_2O_3 film but with a thickness of 200 nm was deposited—in this case at 300 W, 0.67 Pa (5.0 mTorr), and again at room temperature—, but the recorded diffractogram was identical to those presented in **Figure 4**, which means that, for the studied conditions, the amorphous state is independent of the film thickness.

Concerning the chemical characteristics, an XPS analysis was carried out on all the samples with the aim of corroborating that the deposited material corresponds to the desired Al_2O_3, as well as to define the O/Al ratio for each sample. As first results, **Table 2** shows the location of the Al 2*p* and O 1*s* peaks maxima for all the deposited Al_2O_3 thin films before and after 1-min erosion with an argon ion sputtering during the XPS system operation. The locations of these peaks in the binding energy scale, whose mean values are 74.09 and 74.16 eV for the Al 2*p* before and after the erosion with argon ions, respectively, and 531.20 and 531.00 eV for the O 1*s*, also before and after the erosion treatment, fall in the position range compiled by Moulder *et al.* for the Al 2*p* [21b] and O 1*s* [21c] photoelectron lines presented by the Al_2O_3 material. For a better comparison, and as examples for all the measured samples, the XPS spectra obtained before the erosion treatment on the surface of the Al_2O_3 thin films deposited at different pressure at 300 W are plotted in **Figure 5**, while those obtained for the films deposited at different RF power with the deposition pressure fixed at 0.67 Pa (5.0 mTorr) are shown in **Figure 6**. For both cases, all the characteristic XPS signals for aluminum and oxygen are clearly observed.

Furthermore, for the Al_2O_3 thin films deposited at different pressures at 300 W and analyzed before the erosion treatment (presented in **Figure 5)**, it is observed the appearance of argon signals as the deposition pressure decreases. **Figure 5(c)** clearly shows the Ar 2*p* signals, which, among the three pressure values studied, take relevance when the Al_2O_3 thin film is deposited at 0.13 Pa (1.0 mTorr). Depositing the Al_2O_3 thin films at higher pressure values avoided the argon incorporation, as it can be seen in **Figure 6(c)**, in which the Ar 2*p* signals are absent at 0.67 Pa (5.0 mTorr), regardless of the RF power applied. Finally, it is important to mention two important observations regarding the Ar 2*p* signals. First, the location of the centers of the whole Ar 2*p* signals was measured for all the samples that presented residual argon, and resulted in a mean value of 242.05 eV. Second, generally all the measured samples showed a defined peak with maximum at about 241.83 eV, falling exactly in the mean value for the Ar $2p_{3/2}$ photoelectrical line as compiled by Moulder *et al.* for argon implanted in silicon [21d]. Since this last peak was often difficult to identify in the XPS spectra recorded after the erosion treatment with argon ions, we decided to charge-correct these spectra by fixing the centers of the whole Ar 2*p* signals to 242.05 eV, as was calculated for the samples analyzed before the erosion treatment. Thus, the data given previously in **Table 2** for eroded samples were calculated after fixing Ar 2*p* centers to 242.05 eV.

Regarding the deviation from the stoichiometry, **Figure 7** shows the O/Al ratio as a function of RF power at different deposition pressure values. This ratio was calculated from the XPS data recorded before and after the erosion treatment with argon ions. It is observed in the figure that the O/Al ratio decreases with the increase of RF power, but increases with the deposition pressure. Thus, for the studied parameters, the highest excess of oxygen (highest O/Al ratio) was achieved with a RF power of 150 W and a deposition pressure of 0.67 Pa (5.0 mTorr).

3.2. Results of silicon passivation with the sputtering-deposited Al_2O_3

Before addressing the passivation results of the *p*-type *c*-Si wafers obtained with the sputtering-deposited Al_2O_3 thin films, two important points must be considered to help in the discussion of such results. First, it is well-known that the high-energy ions inherent to the sputtering process interact and modify in different ways the substrate surface [26–28]. One of the effects is the generation of lattice defects in the substrate surface, which can be considered a serious damage for surface passivation purposes. However, besides of the increase of Q_f, one of the objectives of the passivation layers is precisely to diminish the interface traps, which seems to be the main problem limiting the level of surface passivation with layers deposited by sputtering. In this regard, the group of Cuevas [15,18] and Chen *et al.* [29] pointed out the importance of finding the proper sputtering parameters that can result in a reduction of the D_{it}. In certain way, this can be considered as a competition against the increase of D_{it} due to the always produced surface damage, inherent to the sputtering technique. On this point, we assume in advance that the increase in RF power and the decrease of deposition pressure, which increases the energy of the particles and the probability to reach the substrate, respectively, lead to an increase in the silicon surface damage. Similar considerations were done by Cuevas and collaborators [15,18].

Second, it is also well-known that the passivation results obtained with the as-deposited Al_2O_3 thin films, regardless of the deposition technique employed, are very poor [2,3]. Therefore, an activation process by applying energy to the material is essential to fully optimize the surface passivation result. For the case of Al_2O_3 deposited by sputtering, it is suggested that such an activation, which is usually achieved by an annealing process, leads to an increase or restructuration of the SiO_x interfacial layer of the formed $Si/SiO_x/Al_2O_3$ structure, which improves both field-effect and chemical passivation by increasing Q_f [15,16,30] and reducing D_{it} [16,30], respectively. Furthermore, the annealing in ambient gasses containing hydrogen results beneficial to passivation due to an extra-reduction of D_{it} by hydrogenation of the silicon dangling bonds or the SiO_x interfacial layer [17,20].

Regarding to the obtained passivation results, **Figure 8** shows the measured τ_{eff} for the *p*-Si wafers uncovered and covered with the 50-nm Al_2O_3 thin films deposited at 300 W and different pressure values. On the other hand, **Figure 9** shows the results obtained with the Al_2O_3 deposited at 0.67 Pa (5.0 mTorr) and different RF power values. These results correspond to both before and after an annealing process at 350 ºC for 20 min with forming gas. In the same way, **Table 3** and **Table 4** show the measured τ_{eff} and calculated S_{eff} values under one-sun illumination for the both previous respective cases; the measured implied open circuit voltage (V_{oc}) is also presented. It can be observed a poor passivation result for all the as-prepared *p*-Si/Al_2O_3 samples, regardless of the argon pressure or the RF power used for depositing the Al_2O_3 thin films, as expected. In the case in which the RF power was varied with the argon pressure fixed at 0.67 Pa (5.0 mTorr), a very slight improvement (although in the bad passivation results range, with τ_{eff} values very close to that measured on the uncovered *p*-Si wafer) is achieved when the Al_2O_3 is deposited at high RF power values. Maybe the energy provided with the increase of this parameter slightly favored the formation or restructuration of the SiO_x interlayer. This change is not appreciable when the argon pressure is varied, maybe indicating that the results are mainly governed by the deposition power.

On the other hand, after the annealing process all the *p*-Si/Al_2O_3 samples reached the maximum passivation improvement, according to their full potential of optimization. It is observed that an increase of the τ_{eff} value—a decrease of S_{eff}—is obtained with the increase of the argon pressure and with a decrease of the RF power used for the deposition of the 50-nm Al_2O_3 thin films. The improved results achieved with the use of such conditions (high pressure and low power) can be related with a decrease in the silicon surface damage, as expected. In the particular case of the argon pressure, higher values also avoided the incorporation of argon into the deposited Al_2O_3 material, although additional studies are necessary to determine the real effect of this contaminant. Thus, among the conditions studied in this work, the best τ_{eff} value at one-sun illumination, 0.34 ms, which corresponds to a S_{eff} of 41.2 cm/s, was obtained after the annealing of the *p*-Si covered with the Al_2O_3 deposited at 150 W and 0.67 Pa (5.0 mTorr).

Although the effect of the argon pressure is evident, the major changes in the passivation results are obtained with the change of the RF power applied during the deposition, thus confirming that the passivation results are governed by the deposition power. In this case, the decrease in the level of passivation with the increase of the RF power surely is associated to an increase of silicon surface damage produced at those conditions, as assumed previously, and also considered by the group of Cuevas [15,18] on the Al_2O_3 deposition by RF sputtering. Furthermore, this decrease in the passivation quality at higher RF power also coincides with the decrease of the O/Al ratio of the Al_2O_3 material, as it was observed in **Figure 7**. A similar correlation can be done with the decrease of the argon pressure, but the incorporation of argon in such conditions complicates a definitive conclusion. However, Li, Cuevas, and collaborators [16] sustained that the surface passivation results are not strongly dependent on the O/Al ratio of the deposited Al_2O_3 material, but on the formation or restructuration of the SiO_x interfacial layer. On the other hand, this correlation between the O/Al ratio and the passivation results is not completely discarded in the review by Dingemans & Kessels [3], and a high O/Al ratio is probably related with the formation of the negative charge, especially if this O/Al ratio is high in the *p*-Si/(SiO_x)/Al_2O_3 interface.

Summarizing the above observations, the best surface passivation obtained at lower RF power and higher argon pressure can be related to a lower damage of the silicon surface, although the effect of the higher O/Al ratio must not be discarded. With the aim of fully corroborate such a correlation, we carried out a simple experiment with an Al_2O_3 thin film grown with deposition conditions that were progressively varied by starting from sputtering conditions that hypothetically lead to minimal surface damage. Such initial deposition conditions were 50 W (corresponding to a power density of 1.1 W/cm^2) and 6.67 Pa (50 mTorr), and the RF power was later gradually increased while the deposition pressure was gradually decreased during the deposition, according to the details tabulated in **Table 5**, which were followed with the objective of increasing the deposition rate and hence the thickness of the passivation film. Here, we assumed that the initial deposited Al_2O_3 material serves mainly as a protective layer for the subsequent more aggressive deposition conditions. By means of this method, we measured a τ_{eff} value of 0.73 ms, corresponding to a S_{eff} equal to 19.2 cm/s, at one-sun illumination after the annealing process at 350 ºC for 20 min with forming gas, thus corroborating all previous assumptions. The measured τ_{eff} as a function of the excess carrier density (Δn) for this sample, compared to the *p*-Si covered with the Al_2O_3 deposited at 150 W and 5.0 mTorr (the best for the series previously discussed), are plotted in **Figure 10**, whereas **Table 6** shows the main data subtracted from the QSSPC measurement for both annealed samples. It is noteworthy that the value of 0.73 ms obtained with this preliminary experiment is to date the best τ_{eff} value reported for *p*-type *c*-Si passivated with Al_2O_3 deposited by sputtering. For a better comparison with the passivation results reported in literature, we show in **Table 7** the best τ_{eff} and S_{eff} recorded at an Δn equal to 1×10^{15} cm^{-3}, for which we obtained a τ_{eff} of 0.85 ms, corresponding to a S_{eff} of 16.5 cm/s, as measured for the sample prepared with minimal surface damage conditions.

3.3. Additional comments and future developments

All the surface passivation results presented in the previous subsection correspond to those values usually obtained under the studied conditions (by methodically following the experimental specifications of the present work). However, we qualitatively noted that considerable variations in the experimental handling of the wafers—such as the cleaning process, exposure time to the air, humidity, and all those experimental errors that obviously must be avoided—lead to a reduction of the surface passivation quality. For example, **Figure 11** shows the different values of surface passivation that can be obtained according to different experimental cares. In this specific case, in which we show the S_{eff} as a function of the studied RF power, it is observed a high variation of the results at higher RF power values due to the mentioned experimental variations. However, the surface passivation is better and easily reproducible when a low RF power is applied for depositing the Al_2O_3 thin films, since under this condition the handling variations did not strongly impact on the passivation results. This is another reason for applying a low RF power to deposit the passivation layers. However, the disadvantage of employing a lower RF power is the reduced deposition rate (see **Figure 1**); therefore, the experimenter must choose the deposition conditions according to the desired results.

By discarding the possible effect of the O/Al ratio (that is, the bulk characteristics of the Al_2O_3 layer) on the surface passivation results, and by considering that the surface damage inherent to the sputtering technique is the main factor that reduces the passivation quality, some interesting passivation schemes can be designed. For example, in this context we assume that a very thin intermediate intrinsic layer of hydrogenated amorphous silicon (*a*-Si:H), deposited by plasma enhanced chemical vapor deposition (PE CVD) before the Al_2O_3 passivation thin film, can serve, on the one hand, as a physical protection layer to the bombardment with the high-energy ions produced during the subsequent sputtering process; and, on the other hand, can serve as a source of hydrogen atoms for surface chemical passivation, in a similar way to the Al_2O_3 deposited by the ALD technique.

Advances in this passivation development, specifically with the *p*-Si/(~6-nm)*a*-Si:H/(50-nm)Al_2O_3 and *n*-Si/(~6-nm)*a*-Si:H/(50-nm)Al_2O_3 structures, in which the Al_2O_3 was deposited at 300 W and 0.67 Pa (5.0 mTorr), were recently presented in the 31st European Photovoltaic Solar Energy Conference and Exhibition (EU PVSEC 2015) [33]. By employing this intrinsic *a*-Si:H interlayer, we achieved, in such preliminary experiments, excellent τ_{eff} values of 1.25 ms (corresponding to a S_{eff} of 11.2 cm/s*) and 1.42 ms (corresponding to a S_{eff} of 9.9 cm/s) for the *p*-Si and *n*-Si wafers, respectively. A systematical study of the use of this intrinsic *a*-Si:H interlayer, as well as experiments to define its main effect on the surface passivation results (either protective layer or hydrogen source), are currently in process.

Summarizing, all the results presented along this paper demonstrate that good surface passivation results can be obtained with solely Al_2O_3 thin films deposited by the industrially suitable sputtering technique, which depend on the deposition conditions. Additionally, there is a good potential to further improve such passivation results.

* In the conference paper [33] we wrongly wrote a S_{eff} of 5.5 cm/s instead of the correct one of 11.2 cm/s.

4. Conclusions

The Al_2O_3 thin films deposited at room temperature by RF magnetron sputtering are amorphous and highly transparent, independently of the RF power and argon deposition pressure, and even regardless of the film thickness.

The deposition of Al_2O_3 thin films at low argon pressure values can result in an incorporation of argon into the deposited films. This is evident for Al_2O_3 deposited at 0.13 Pa (1.0 mTorr), whereas the incorporation of argon at 0.67 Pa (5.0 mTorr) was not detected.

The O/Al ratio of the Al_2O_3 material increased with the deposition pressure and with the decrease of the RF power applied. Among the studied parameters, the highest O/Al ratio was obtained at 0.67 Pa (5.0 mTorr) and 150 W.

Bad surface passivation results were obtained with the as-deposited Al_2O_3 thin films, but they considerably improved after an annealing process, which is usually attributed to the formation or restructuration of a SiO_x interlayer, leading to an increase of Q_f and a decrease of D_{it}. The different surface passivation results obtained after the annealing process indicate that each sample shows a different potential of passivation, which depends on the overall deposition conditions.

The best surface passivation results are obtained by applying a low RF power and high argon pressure for depositing the Al_2O_3 thin films, which is attributed to a reduction of the surface damage inherent to the sputtering technique. Also, a probable effect of the higher O/Al ratio is not discarded.

Among the studied parameters, the best τ_{eff} value, 0.34 ms, which corresponds to an S_{eff} of 41 cm/s, is obtained after an annealing with forming gas at 350 ºC for 20 min (parameters nor studied nor optimized in this work) applied to the *p*-Si covered with 50-nm Al_2O_3 deposited at 150 W and 0.67 Pa (5.0 mTorr).

A simple experiment by employing a passivation film of Al_2O_3 deposited at initial very high argon pressure, 6.67 Pa (50 mTorr), and low RF power, 50 W, assumed as conditions that lead a minimal surface damage, provided a τ_{eff} value of 0.73 ms (a S_{eff} of 19 cm/s), thus corroborating that the silicon surface damage can be diminished with the proper sputtering conditions: high power and low pressure.

Therefore, the magnetron sputtering technique, which is nowadays completely integrated into the industry, is suitable for depositing Al_2O_3 passivation layers with good enough silicon surface passivation properties.

Acknowledgments

The *Centres Científics i Tecnològics de la Universitat de Barcelona* (CCiTUB) are acknowledged for the XRD and XPS measurements. The authors acknowledge the financial support by the Spanish *Ministerio de Economía y Competitividad* (MINECO) through the projects ENE2013-48629-C4-1-R and ENE2013-48629-C4-2-R, and Jorge Alberto García-Valenzuela gratefully acknowledges the financial support by the Mexican *Consejo Nacional de Ciencia y Tecnología* (CONACyT) with registration numbers 208159 and 251082.

References

[1] B. Hoex, J. Schmidt, P. Pohl, M.C.M. van de Sanden, W.M.M. Kessels, Silicon surface passivation by atomic layer deposited Al_2O_3, J. Appl. Phys. 104 (4) (2008) 044903.

[2] G. Dingemans, W.M.M. Kessels, Recent progress in the development and understanding of silicon surface passivation by aluminum oxide for photovoltaics, EU PVSEC Proceedings, 2010, pp. 1083–1090; presented at: 25th European Photovoltaic Solar Energy Conference and Exhibition / 5th World Conference on Photovoltaic Energy Conversion (25th EU PVSEC / WCPEC-5), Valencia, Valencian Community, Spain, September 6–10, 2010.

[3] G. Dingemans, W.M.M. Kessels, Status and prospects of Al_2O_3-based surface passivation schemes for silicon solar cells, J. Vac. Sci. Technol. A 30 (4) (2012) 040802.

[4] M.Z. Rahman, S.I. Khan, Advances in surface passivation of c-Si solar cells, Mater. Renew. Sustain. Energy 1 (1) (2012) 1:1.

[5] S. Xiao, S. Xu, Status and progress of high-efficiency silicon solar cells, in: X. Wang, Z.M. Wang (Eds.), High-Efficiency Solar Cells — Physics, Materials, and Devices, Springer Series in Material Sciences, Volume 190, Springer Science+Business Media, 2014, pp. 1–58.

[6] G. Hahn, S. Joos, State-of-the-art industrial crystalline silicon solar cells, in: G.P. Willeke, E.R. Weber (Eds.), Semiconductors and Semimetals (Volume 90) — Advances in Photovoltaics: Part 3, Elsevier Inc., 2014, pp. 1–72.

[7] N. Balaji, S.Q. Hussain, C. Park, J. Raja, J. Yi, R. Jeyakumar, Surface passivation schemes for high-efficiency c-Si solar cells - A review, Trans. Electr. Electron. Mater. 16 (5) (2015) 227–233.

[8] J. Schmidt, F. Werner, B. Veith, D. Zielke, R. Bock, V. Tiba, P. Poodt, F. Roozeboom, [T.-T.]A. Li, A. Cuevas, R. Brendel, Industrially relevant Al_2O_3 deposition techniques for the surface passivation of Si solar cells, EU PVSEC Proceedings, 2010, pp. 1130–1133; presented at: 25th European Photovoltaic Solar Energy Conference and Exhibition / 5th World Conference on Photovoltaic Energy Conversion (25th EU PVSEC / WCPEC-5), Valencia, Valencian Community, Spain, September 6–10, 2010.

[9] J. Schmidt, F. Werner, B. Veith, D. Zielke, R. Bock, R. Brendel, V. Tiba, P. Poodt, F. Roozeboom, [T.-T.]A. Li, A. Cuevas, Surface passivation of silicon solar cells using industrially relevant Al_2O_3 deposition techniques, Photovoltaics International, Technical Papers, Edition 10 (2011) 52–57.

[10] J. Schmidt, F. Werner, B. Veith, D. Zielke, S. Steingrube, P.P. Altermatt, S. Gatz, T. Dullweber, R. Brendel, Advances in the surface passivation of silicon solar cells, Energy Procedia 15 (2012) 30–39.

[11] P. Saint-Cast, M. Hofmann, S. Kühnhold, D. Kania, L. Weiss, Y.-H. Heo, E. Billot, P. Olwal, D. Trogus, J. Rentsch, R. Preu, A review of PECVD aluminum oxide for surface passivation, EU PVSEC Proceedings, 2012, pp. 1797–1801; presented at: 27th European Photovoltaic Solar Energy Conference and Exhibition (27th EU PVSEC), Frankfurt, Hesse, Germany, September 24–28, 2012.

[12] G. Agostinelli, A. Delabie, P. Vitanov, Z. Alexieva, H.F.W. Dekkers, S. De Wolf, G. Beaucarne, Very low surface recombination velocities on p-type silicon wafers passivated with a dielectric with fixed negative charge, Sol. Energy Mater. Sol. Cells 90 (18–19) (2006) 3438–3443.

[13] B. Hoex, S.B.S. Heil, E. Langereis, M.C.M. van de Sanden, W.M.M. Kessels, Ultralow surface recombination of *c*-Si substrates passivated by plasma-assisted atomic layer deposited Al_2O_3, Appl. Phys. Lett. 89 (4) (2006) 042112.

[14] F. Werner, W. Stals, R. Görtzen, B. Veith, R. Brendel, J. Schmidt, High-rate atomic layer deposition of Al_2O_3 for the surface passivation of Si solar cells, Energy Procedia 8 (2011) 301–306.

[15] T.-T.[A.] Li, A. Cuevas, Effective surface passivation of crystalline silicon by rf sputtered aluminum oxide, phys. status solidi RRL 3 (5) (2009) 160–162.

[16] T.-T.A. Li, S. Ruffell, M. Tucci, Y. Mansoulié, C. Samundsett, S. De Iullis, L. Serenelli, A. Cuevas, Influence of oxygen on the sputtering of aluminum oxide for the surface passivation of crystalline silicon, Sol. Energy Mater. Sol. Cells 95 (1) (2011) 69–72.

[17] T.-T.A. Li, A. Cuevas, Role of hydrogen in the surface passivation of crystalline silicon by sputtered aluminum oxide, Prog. Photovolt: Res. Appl. 19 (3) (2011) 320–325.

[18] X. Zhang, A. Cuevas, A. Thomson, Process control of reactive sputter deposition of AlO_x and improved surface passivation of crystalline silicon, IEEE J. Photovolt. 3 (1) (2013) 183–188.

[19] X. Zhang, A. Cuevas, Plasma hydrogenated, reactively sputtered aluminum oxide for silicon surface passivation, phys. status solidi RRL 7 (9) (2013) 619–622.

[20] X. Zhang, A. Thomson, A. Cuevas, Silicon surface passivation by sputtered aluminum oxide: influence of annealing temperature and ambient gas, ECS Solid State Lett. 3 (11) (2014) N37–N39.

[21] J.F. Moulder, W.F. Stickle, P.E. Sobol, K.D. Bomben, in: J. Chastain, R.C. King Jr. (Eds.), Handbook of X-Ray Photoelectron Spectroscopy — A Reference Book of Standard Spectra for Identification and Interpretation of XPS Data, Physical Electronics, Inc., Eden Praire, Minnesota, USA, 1995, pp. (a) 14,22,33, (b) 54,55, (c) 44,45, (d) 64,65.

[22] W. Kern, D.A. Puotinen, Cleaning solutions based on hydrogen peroxide for use in silicon semiconductor technology, RCA Review 31 (1970) 187–206.

[23] W. Kern, The evolution of silicon wafer cleaning technology, J. Electrochem. Soc. 137 (6) (1990) 1887–1892.

[24] A.G. Aberle, Crystalline Silicon Solar Cells — Advanced Surface Passivation and Analysis, Centre for Photovoltaic Engineering, University of New South Wales, Sidney, Australia, 1999, pp. (a) 75, (b) 53.

[25] J. Schmidt, A.G. Aberle, Accurate method for the determination of bulk minority-carrier lifetimes of mono- and multicrystalline silicon wafers, J. Appl. Phys. 81 (9) (1997) 6186–6199.

[26] D.M. Mattox, Particle bombardment effects on thin-film deposition: A review, J. Vac. Sci. Technol. A 7 (3) (1989) 1105–1114.

[27] M. Ohring, Discharges, plasmas, and ion-surface interactions, in: Materials Science of Thin Films, 2nd Ed., Academic Press, 2001, pp. 145–202.

[28] D.M. Mattox, Physical sputtering and sputter deposition (Sputtering), in: Handbook of Physical Vapor Deposition (PVD) Processing, 2nd Ed., Elsevier Inc., 2010, pp. 237–286.

[29] S. Chen, L. Tao, L. Zeng, R. Hong, RF magnetron sputtering aluminum oxide film for surface passivation on crystalline silicon wafers, Int. J. Photoenergy 2013 (2013) 792357.

[30] M. Bhaisare, A. Misra, A. Kottantharayil, Aluminum oxide deposited by pulsed-DC reactive sputtering for crystalline silicon surface passivation, IEEE J. Photovolt. 3 (3) (2013) 930–935.

[31] M. Bhaisare, D. Sutar, A. Misra, A. Kottantharayil, Effect of power density on the passivation quality of pulsed - DC reactive sputtered aluminium oxide on p - type crystalline silicon, 2013

IEEE 39th Photovoltaic Specialists Conference (PVSC), 2013, pp. 1207–1211; presented at: 2013 IEEE 39th Photovoltaic Specialists Conference (PVSC), Tampa, Florida, USA, June 16–21, 2013.

[32] R. Kotipalli, R. Delamare, F. Henry, J. Proost, D. Flandre, Thermal stability analysis of DC-sputtered Al_2O_3 films for surface passivation of c-Si solar cells, EU PVSEC Proceedings, 2013, pp. 1278–1281; presented at: 28th European Photovoltaic Solar Energy Conference and Exhibition (28th EU PVSEC), Paris, France, September 30 – October 4, 2013.

[33] J.A. García-Valenzuela, Á. Caballero, J.M. Asensi, J. Bertomeu, J. Andreu, L.G. Gerling-Sarabia, A.B. Morales[-Vilches], P. Ortega, C. Voz, Intermediate amorphous silicon layer for crystalline silicon passivation with alumina, EU PVSEC Proceedings, 2015, pp. 719–723; presented at: 31st European Photovoltaic Solar Energy Conference and Exhibition (EU PVSEC 2015), Hamburg, Germany, September 14–18, 2015.

Table captions

Table 1. Integrated percent transmittance calculated in the interval from 400 to 1100 nm for the Al_2O_3 thin films deposited on glass substrate at different RF power and deposition pressure values; the integrated percent transmittance value calculated for the glass substrate is 94.1%.

Table 2. Binding energy positions of the Al 2*p* and O 1*s* peaks maxima for the Al_2O_3 deposited on glass substrate at different RF power and deposition pressure; values at the left of the arrow correspond to the Al_2O_3 surface as is, while values at the right correspond to those recorded after 1-min erosion with argon ion sputtering.

Table 3. Effective lifetime, effective surface recombination velocity, and implied open circuit voltage values measured or calculated under one-sun illumination for the as-prepared and annealed *p*-Si/Al_2O_3 samples obtained at different argon pressure values at a RF power of 300 W; the bare *p*-Si wafer data are also included for comparison.

Table 4. Effective lifetime, effective surface recombination velocity, and implied open circuit voltage values measured or calculated under one-sun illumination for the as-prepared and annealed *p*-Si/Al_2O_3 samples obtained at different RF power values at a deposition pressure of 0.67 Pa (5.0 mTorr); the bare *p*-Si wafer data are also included for comparison.

Table 5. Details for the conditions followed to progressively depositing Al_2O_3 starting from minimal surface damage conditions.

Table 6. Effective lifetime, effective surface recombination velocity, and implied open circuit voltage values measured or calculated under one-sun illumination for the annealed *p*-Si samples covered with the Al_2O_3 thin films deposited at 150 W and 0.67 Pa (5.0 mTorr), for the first case, and under minimal surface damage conditions, for the second case.

Table 7. Best effective lifetime and surface recombination velocity values obtained on annealed *p*-type *c*-Si wafers passivated with Al_2O_3 deposited by sputtering (under conditions without intentionally added hydrogen), according to the reported in literature for an excess carrier density of 1×10^{15} cm^{-3}.

Figure captions

Figure 1. Variation of the calculated deposition rate of the Al_2O_3 thin films as a function of RF power for different deposition pressure values, by using mechanically and optically measured data.

Figure 2. Percent transmittance and percent reflectance spectra of the glass substrates uncovered and covered with the Al_2O_3 thin films deposited at different pressure values at a RF power of 300 W.

Figure 3. Percent transmittance and percent reflectance spectra of the glass substrates uncovered and covered with the Al_2O_3 thin films deposited at different RF power values at a deposition pressure of 0.67 Pa (5.0 mTorr).

Figure 4. X-ray diffractograms of the Al_2O_3 thin films deposited on glass substrate at different RF power values at a deposition pressure of 0.67 Pa (5.0 mTorr).

Figure 5. X-ray photoelectron spectra of the non-eroded Al_2O_3 thin films deposited on glass substrate at different pressure values at a RF power of 300 W for (a) the survey interval, (b) the high-resolution O 1*s* region, (c) the Ar 2*p* region, and (d) the high-resolution Al 2*p* region.

Figure 6. X-ray photoelectron spectra of the non-eroded Al_2O_3 thin films deposited on glass substrate at different RF power values at a deposition pressure of 0.67 Pa (5.0 mTorr) for (a) the survey interval, (b) the high-resolution O 1*s* region, (c) the Ar 2*p* region, and (d) the high-resolution Al 2*p* region.

Figure 7. Variation of O/Al ratio of the Al_2O_3 material as a function of RF power for different deposition pressure values, calculated from the X-ray photoelectron spectroscopy data measured before and after the 1-min erosion treatment with an argon ion sputtering.

Figure 8. Variation of effective lifetime of the as-prepared and annealed *p*-Si samples uncovered and covered with the Al_2O_3 thin films deposited at different argon pressure values at a RF power of 300 W, expressed as a function of the excess carrier density.

Figure 9. Variation of effective lifetime of the as-prepared and annealed *p*-Si samples uncovered and covered with the Al_2O_3 thin films deposited at different RF power values at a deposition pressure of 0.67 Pa (5.0 mTorr), expressed as a function of the excess carrier density.

Figure 10. Variation of effective lifetime of the annealed *p*-Si samples uncovered and covered with the Al_2O_3 thin films deposited at 150 W and 0.67 Pa (5.0 mTorr), for one case, and under minimal surface damage conditions, for the best case.

Figure 11. Variation of the effective surface recombination velocity due to certain changes in the experimental handling; the results, which must not be confused as statistical ones, are plotted as a function of RF power and correspond to those calculated after the annealing treatment.

Table 1. Integrated percent transmittance calculated in the interval from 400 to 1100 nm for the Al_2O_3 thin films deposited on glass substrate at different RF power and deposition pressure values; the integrated percent transmittance value calculated for the glass substrate is 94.1%.

RF power (W)	Deposition pressure (Pa)	Recorded DC bias voltage (V)	Integrated percent transmittance, *%T* (%)
150	0.13 (1.0 mTorr)	60–40	90.8
150	0.33 (2.5 mTorr)	61–43	91.3
150	0.67 (5.0 mTorr)	62–45	91.6
300	0.13 (1.0 mTorr)	172–150	91.2
300	0.33 (2.5 mTorr)	152–138	91.4
300	0.67 (5.0 mTorr)	160–150	91.8
450	0.13 (1.0 mTorr)	271–263	91.5
450	0.33 (2.5 mTorr)	220–211	91.7
450	0.67 (5.0 mTorr)	231–225	91.8

Table 2. Binding energy positions of the Al 2*p* and O 1*s* peaks maxima for the Al_2O_3 deposited on glass substrate at different RF power and deposition pressure; values at the left of the arrow correspond to the Al_2O_3 surface as is, while values at the right correspond to those recorded after 1-min erosion with argon ion sputtering.

RF power (W)	Deposition pressure (Pa)	Al 2*p* peak position (eV)	O 1*s* peak position (eV)
150	0.13 (1.0 mTorr)	74.12 → 74.18	531.18 → 530.98
150	0.67 (5.0 mTorr)	74.08 → 74.18	531.37 → 531.15
300	0.13 (1.0 mTorr)	74.14 → 74.16	531.34 → 531.14
300	0.33 (2.5 mTorr)	74.00 → 74.22	531.09 → 530.93
300	0.67 (5.0 mTorr)	74.06 → 74.11	531.25 → 530.86
450	0.13 (1.0 mTorr)	74.15 → 74.15	531.07 → 530.99
450	0.67 (5.0 mTorr)	74.09 → 74.11	531.13 → 530.94

Table 3. Effective lifetime, effective surface recombination velocity, and implied open circuit voltage values measured or calculated under one-sun illumination for the as-prepared and annealed *p*-Si/Al_2O_3 samples obtained at different argon pressure values at a RF power of 300 W; the bare *p*-Si wafer data are also included for comparison.

Sample	Effective lifetime, τ_{eff} (μs)		Effective surface recombination velocity, S_{eff} (cm/s)		Implied open circuit voltage, V_{oc} (mV)	
	As-prepared	Annealed	As-prepared	Annealed	As-prepared	Annealed
p-Si	~0.7	–	$>2.1\times10^4$	–	514	–
p-Si/Al_2O_3 at 0.13 Pa, 140–119 V	~1.0	173	$>1.4\times10^4$	80.9	519	654
p-Si/Al_2O_3 at 0.33 Pa, 134–116 V	~1.1	185	$>1.3\times10^4$	75.7	519	656
p-Si/Al_2O_3 at 0.67 Pa, 152–133 V	~1.1	275	$>1.3\times10^4$	51.0	520	675

Table 4. Effective lifetime, effective surface recombination velocity, and implied open circuit voltage values measured or calculated under one-sun illumination for the as-prepared and annealed *p*-Si/Al_2O_3 samples obtained at different RF power values at a deposition pressure of 0.67 Pa (5.0 mTorr); the bare *p*-Si wafer data are also included for comparison.

Sample	Effective lifetime, τ_{eff} (μs)		Effective surface recombination velocity, S_{eff} (cm/s)		Implied open circuit voltage, V_{oc} (mV)	
	As-prepared	Annealed	As-prepared	Annealed	As-prepared	Annealed
p-Si	~0.7	–	$>2.1\times10^4$	–	514	–
p-Si/Al_2O_3 at 150 W, 48–25 V	~0.8	340	$>1.8\times10^4$	41.2	515	682
p-Si/Al_2O_3 at 300 W, 134–109 V	~0.9	275	$>1.5\times10^4$	51.0	520	675
p-Si/Al_2O_3 at 450 W, 221–192 V	~1.5	135	$>0.9\times10^4$	104	536	652

Table 5. Details for the conditions followed to progressively depositing Al_2O_3 starting from minimal surface damage conditions.

RF power (W)	Deposition pressure (Pa)	Time (min)	Accumulated time (min)
50	6.67 (50.0 mTorr)	5	5
50	5.33 (40.0 mTorr)	25	30
50 – 60	5.33 – 4.00 (40.0 – 30.0 mTorr)	2	32
60	4.00 (30.0 mTorr)	5	37
60 – 70	4.00 – 2.67 (30.0 – 20.0 mTorr)	2	39
70	2.67 (20.0 mTorr)	5	44
70 – 80	2.67 – 2.00 (20.0 – 15.0 mTorr)	2	46
80	2.00 (15.0 mTorr)	3	49
80 – 90	2.00 – 0.93 (15.0 – 7.0 mTorr)	2	51
90	0.93 (7.0 mTorr)	2	53
90 – 100	0.93 – 0.67 (7.0 – 5.0 mTorr)	2	55
100	0.67 (5.0 mTorr)	2	57
100 – 150	0.67 (5.0 mTorr)	8	65
150	0.67 (5.0 mTorr)	55	120

Table 6. Effective lifetime, effective surface recombination velocity, and implied open circuit voltage values measured or calculated under one-sun illumination for the annealed *p*-Si samples covered with the Al_2O_3 thin films deposited at 150 W and 0.67 Pa (5.0 mTorr), for the first case, and under minimal surface damage conditions, for the second case.

Sample	Effective lifetime, τ_{eff} (μs)	Effective surface recombination velocity, S_{eff} (cm/s)	Implied open circuit voltage, V_{oc} (mV)
p-Si/Al_2O_3 at 150 W and 5.0 mTorr	340	41.2	682
p-Si/Al_2O_3 at minimal surface damage	728	19.2	708

Table 7. Best effective lifetime and surface recombination velocity values obtained on annealed *p*-type *c*-Si wafers passivated with Al_2O_3 deposited by sputtering (under conditions without intentionally added hydrogen), according to the reported in literature for an excess carrier density of 1×10^{15} cm^{-3}.

Year, authors	Target	Annealing conditions	Effective lifetime, τ_{eff} (μs)	Effective surface recombination velocity, S_{eff} (cm/s)
2009, Li & Cuevas [15]	Al	N_2, 400 ºC, 60 min	227 [a]	74 [b]
2009, Li & Cuevas [15]	Al	Forming gas, 400 ºC, 60 min	292 [a]	55 [b]
2010, Schmidt, Li, Cuevas, *et al.* [8]	Al	400±50 ºC, 15 min	425 [a]	35 [b]
2011, Schmidt, Li, Cuevas, *et al.* [9]	Al	400±50 ºC, 15 min	425 [a]	35 [b]
2011, Li, Cuevas, *et al.* [16]	Al	N_2, 400 ºC, 180 min	212 [c]	73 [a]
2012, Schmidt *et al.* [10]	Al	400±50 ºC, 15 min	425 [a]	35 [b]
2013, Chen *et al.* [29]	Al	N_2, 500 ºC, 30 min	135 [b]	-
2013, Bhaisare *et al.* [30]	Al	N_2 or N_2+O_2, 520 ºC	324 [a]	44 [a]
2013, Bhaisare *et al.* [31]	Al	N_2+O_2, 520 ºC	390 [a]	38 [a]
2013, Kotipalli *et al.* [32]	Al	Forming gas, 430 ºC, 30 min	49 [a]	200 [c]
2015, García-Valenzuela *et al.* [33]	Al_2O_3	Forming gas, 350 ºC, 20 min	46 [a,d]	307 [a,d]
2016, García-Valenzuela *et al.*, this work	Al_2O_3	Forming gas, 350 ºC, 20 min	851 [d]	16.5 [d]

[a] Value subtracted from the plots reported in the paper.

[b] Value numerically reported in the paper.

[c] Value calculated from data given in the paper.

[d] Value given as a preliminary result.

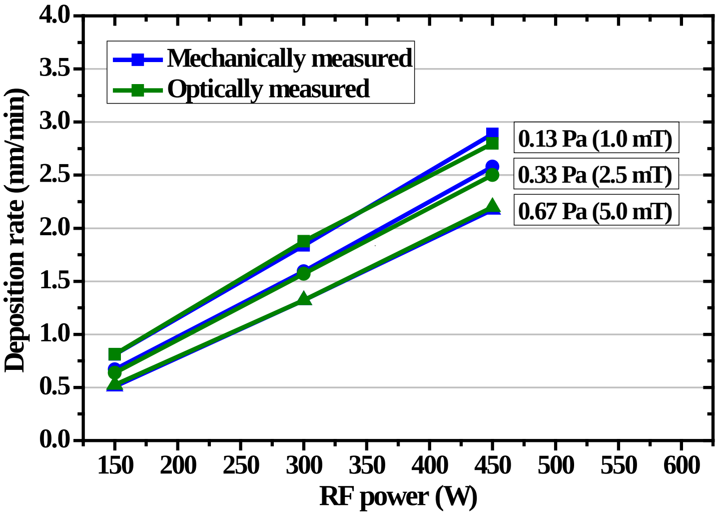
Mechanically measured
Optically measured
0.13 Pa (1.0 mT)
0.33 Pa (2.5 mT)
0.67 Pa (5.0 mT)
Deposition rate (nm/min)
4.0
3.5
3.0
2.5
2.0
1.5
1.0
0.5
0.0
150
200
250
300
350
400
450
500
550
600
RF power (W)

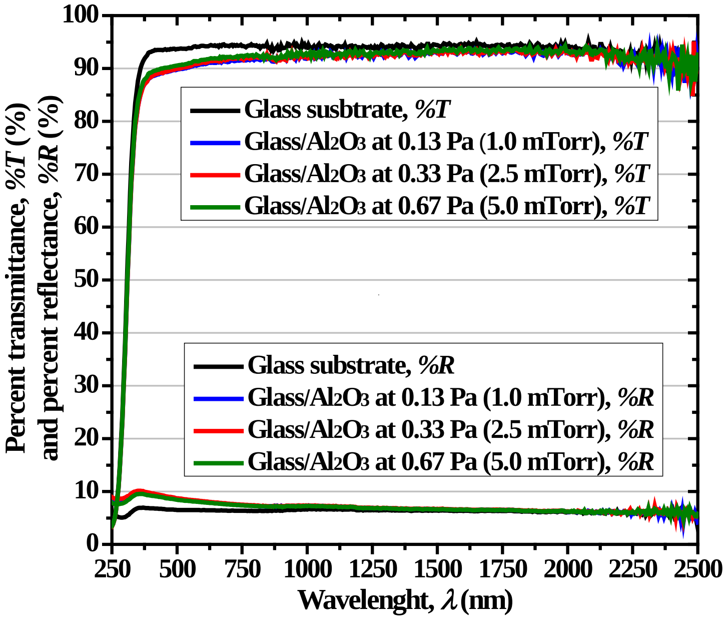
Percent transmittance, %*T* (%)
and percent reflectance, %*R* (%)
100
90
80
70
60
50
40
30
20
10
0
250
500
750
1000
1250
1500
1750
2000
2250
2500
Wavelenght, λ (nm)
Glass susbtrate, %*T*
Glass/Al_2O_3 at 0.13 Pa (1.0 mTorr), %*T*
Glass/Al_2O_3 at 0.33 Pa (2.5 mTorr), %*T*
Glass/Al_2O_3 at 0.67 Pa (5.0 mTorr), %*T*
Glass substrate, %*R*
Glass/Al_2O_3 at 0.13 Pa (1.0 mTorr), %*R*
Glass/Al_2O_3 at 0.33 Pa (2.5 mTorr), %*R*
Glass/Al_2O_3 at 0.67 Pa (5.0 mTorr), %*R*

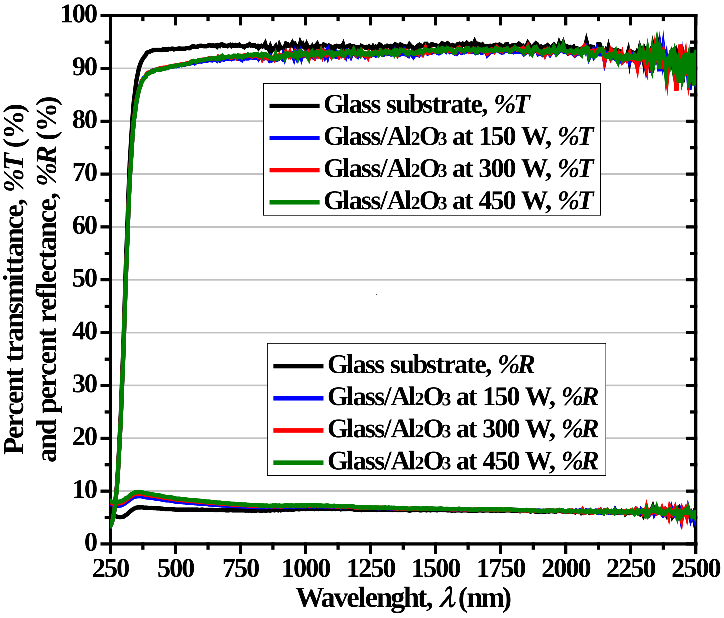
Percent transmittance, %T (%)
and percent reflectance, %R (%)
Wavelenght, λ (nm)
0
10
20
30
40
50
60
70
80
90
100
250
500
750
1000
1250
1500
1750
2000
2250
2500
Glass substrate, %T
Glass/Al_2O_3 at 150 W, %T
Glass/Al_2O_3 at 300 W, %T
Glass/Al_2O_3 at 450 W, %T
Glass substrate, %R
Glass/Al_2O_3 at 150 W, %R
Glass/Al_2O_3 at 300 W, %R
Glass/Al_2O_3 at 450 W, %R

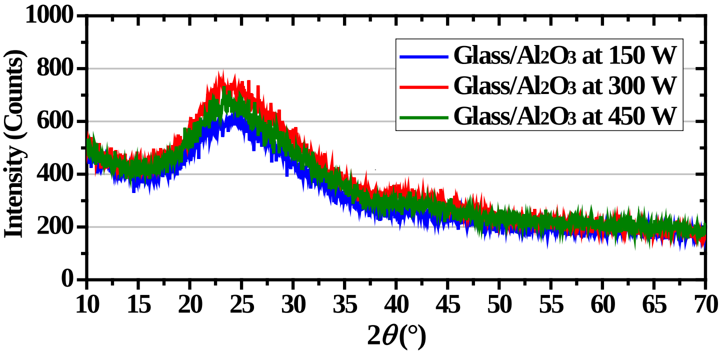
Intensity (Counts)
1000
800
600
400
200
0
10
15
20
25
30
35
40
45
50
55
60
65
70
2θ(°)
Glass/Al2O3 at 150 W
Glass/Al2O3 at 300 W
Glass/Al2O3 at 450 W

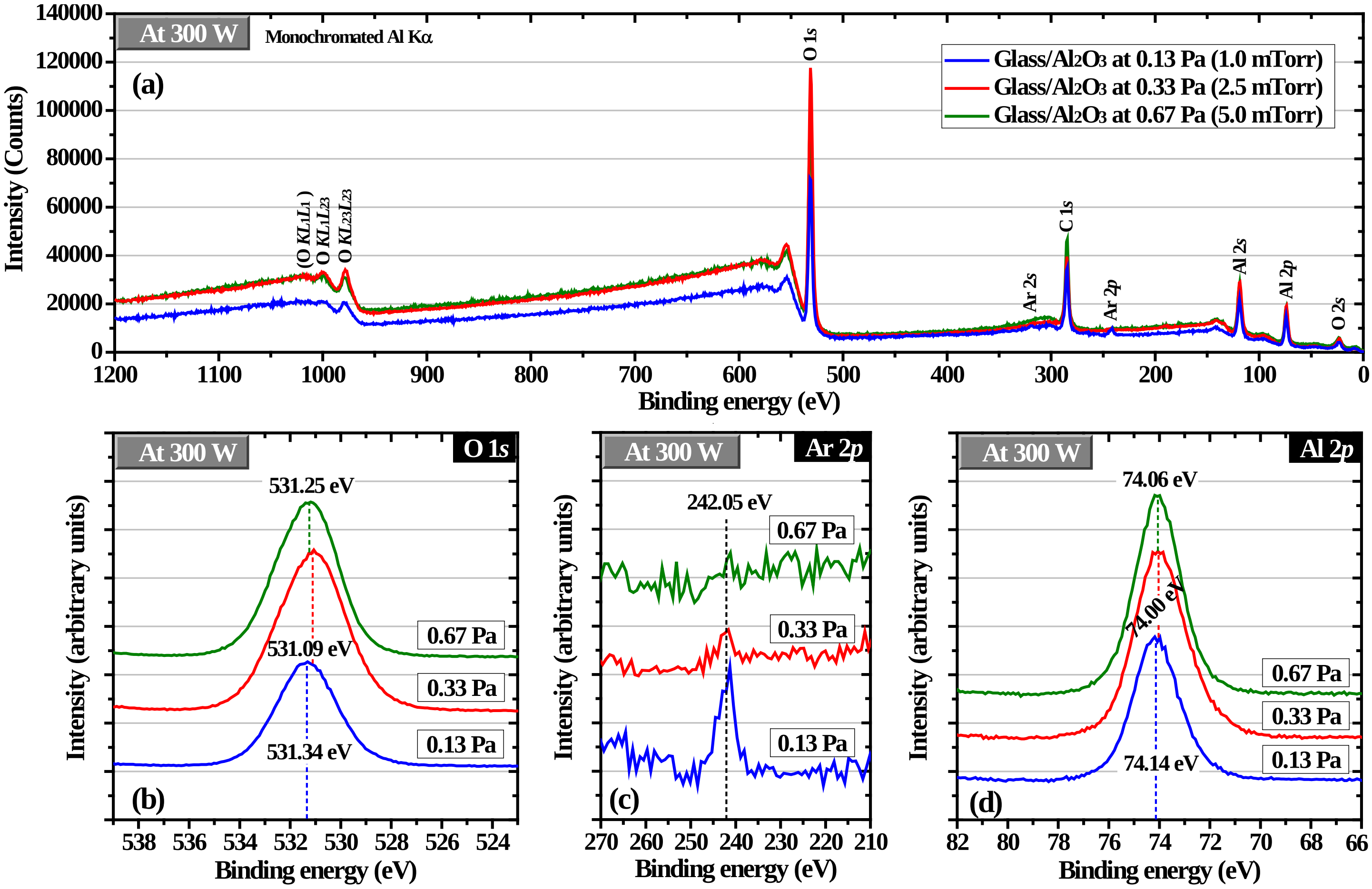
At 300 W
Monochromated Al Kα
(a)
Intensity (Counts)
140000
120000
100000
80000
60000
40000
20000
0
Glass/Al2O3 at 0.13 Pa (1.0 mTorr)
Glass/Al2O3 at 0.33 Pa (2.5 mTorr)
Glass/Al2O3 at 0.67 Pa (5.0 mTorr)
(O KL1L1)
O KL1L23
O KL23L23
O 1s
Ar 2s
C 1s
Ar 2p
Al 2s
Al 2p
O 2s
1200
1100
1000
900
800
700
600
500
400
300
200
100
0
Binding energy (eV)
At 300 W
O 1s
531.25 eV
531.09 eV
531.34 eV
0.67 Pa
0.33 Pa
0.13 Pa
(b)
Intensity (arbitrary units)
538
536
534
532
530
528
526
524
Binding energy (eV)
At 300 W
Ar 2p
242.05 eV
0.67 Pa
0.33 Pa
0.13 Pa
(c)
Intensity (arbitrary units)
270
260
250
240
230
220
210
Binding energy (eV)
At 300 W
Al 2p
74.06 eV
74.00 eV
74.14 eV
0.67 Pa
0.33 Pa
0.13 Pa
(d)
Intensity (arbitrary units)
82
80
78
76
74
72
70
68
66
Binding energy (eV)

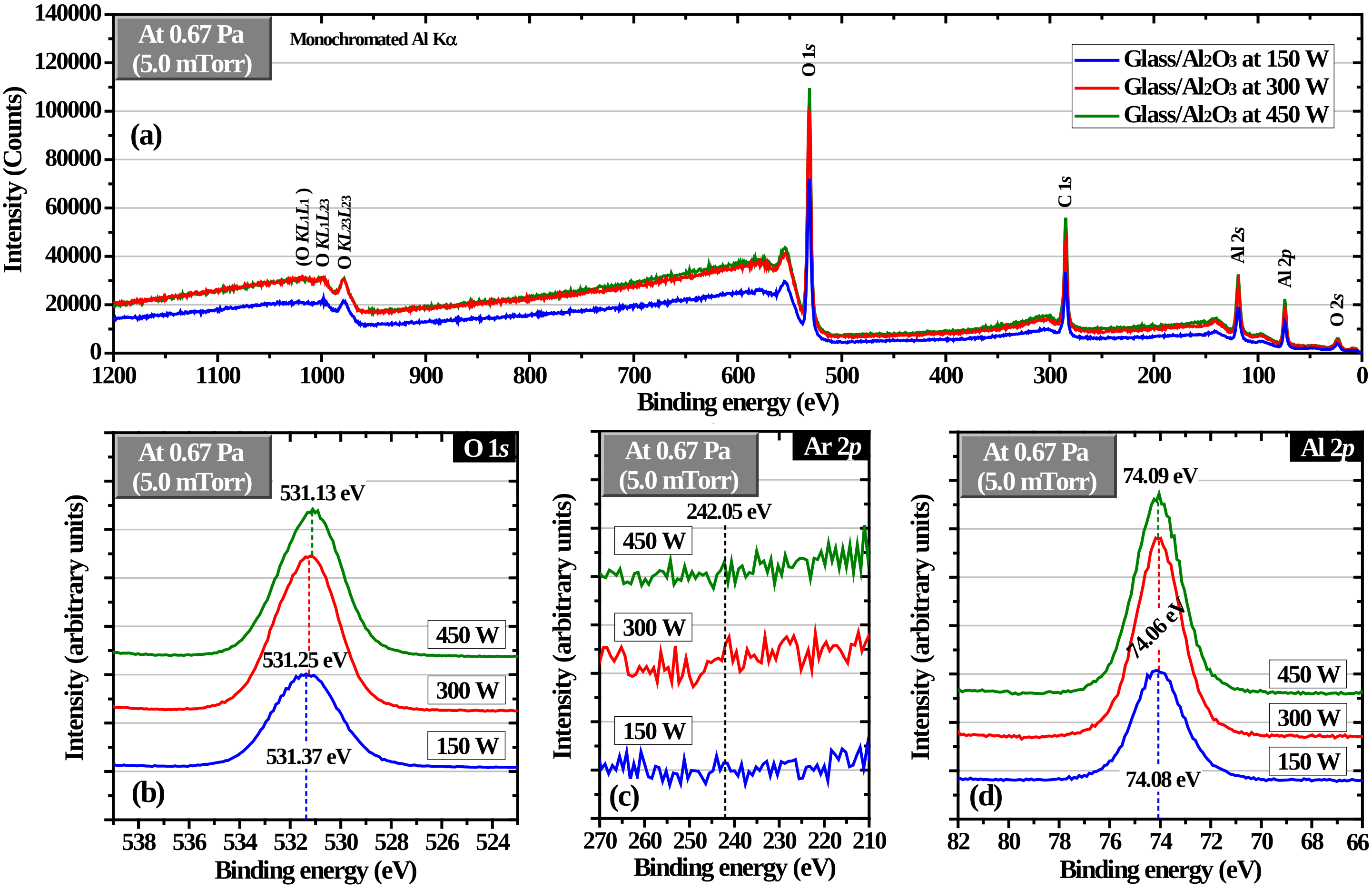

At 0.67 Pa (5.0 mTorr)
Monochromated Al Kα
(a)
Intensity (Counts)
140000
120000
100000
80000
60000
40000
20000
0
(O KL1L1)
O KL1L23
O KL23L23
O 1s
C 1s
Al 2s
Al 2p
O 2s
Glass/Al2O3 at 150 W
Glass/Al2O3 at 300 W
Glass/Al2O3 at 450 W
1200
1100
1000
900
800
700
600
500
400
300
200
100
0
Binding energy (eV)
At 0.67 Pa (5.0 mTorr)
O 1s
531.13 eV
531.25 eV
531.37 eV
450 W
300 W
150 W
(b)
Intensity (arbitrary units)
538
536
534
532
530
528
526
524
Binding energy (eV)
At 0.67 Pa (5.0 mTorr)
Ar 2p
242.05 eV
450 W
300 W
150 W
(c)
Intensity (arbitrary units)
270
260
250
240
230
220
210
Binding energy (eV)
At 0.67 Pa (5.0 mTorr)
Al 2p
74.09 eV
74.06 eV
74.08 eV
450 W
300 W
150 W
(d)
Intensity (arbitrary units)
82
80
78
76
74
72
70
68
66
Binding energy (eV)

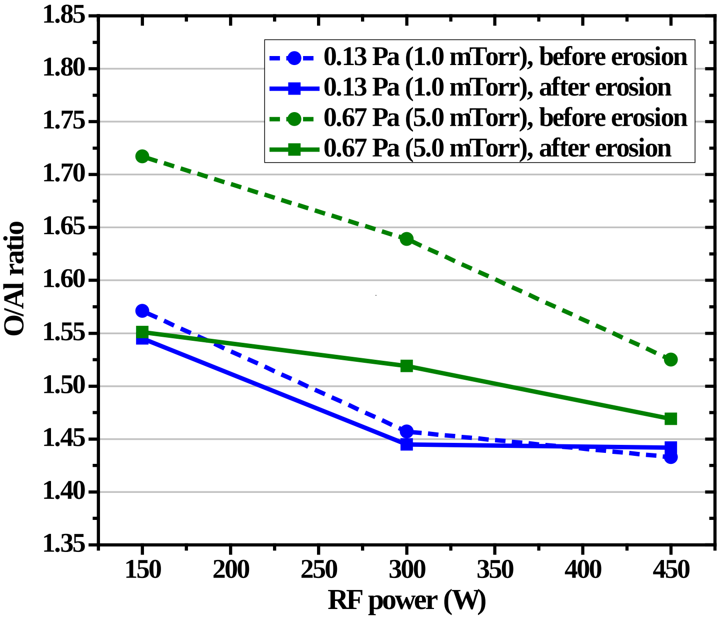
1.85
1.80
1.75
1.70
1.65
1.60
1.55
1.50
1.45
1.40
1.35
O/Al ratio
150
200
250
300
350
400
450
RF power (W)
0.13 Pa (1.0 mTorr), before erosion
0.13 Pa (1.0 mTorr), after erosion
0.67 Pa (5.0 mTorr), before erosion
0.67 Pa (5.0 mTorr), after erosion

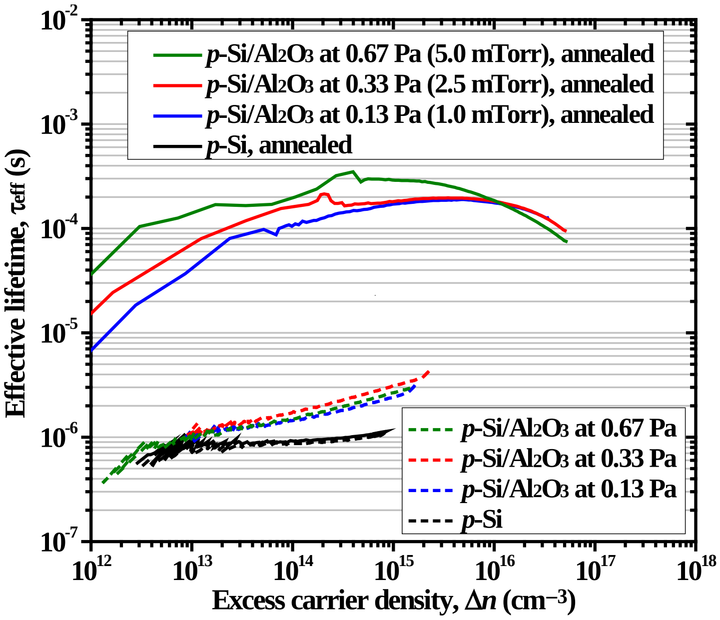
10^{-2}
10^{-3}
10^{-4}
10^{-5}
10^{-6}
10^{-7}
Effective lifetime, τ_{eff} (s)
10^{12}
10^{13}
10^{14}
10^{15}
10^{16}
10^{17}
10^{18}
Excess carrier density, Δn (cm^{-3})
p-Si/Al_2O_3 at 0.67 Pa (5.0 mTorr), annealed
p-Si/Al_2O_3 at 0.33 Pa (2.5 mTorr), annealed
p-Si/Al_2O_3 at 0.13 Pa (1.0 mTorr), annealed
p-Si, annealed
p-Si/Al_2O_3 at 0.67 Pa
p-Si/Al_2O_3 at 0.33 Pa
p-Si/Al_2O_3 at 0.13 Pa
p-Si

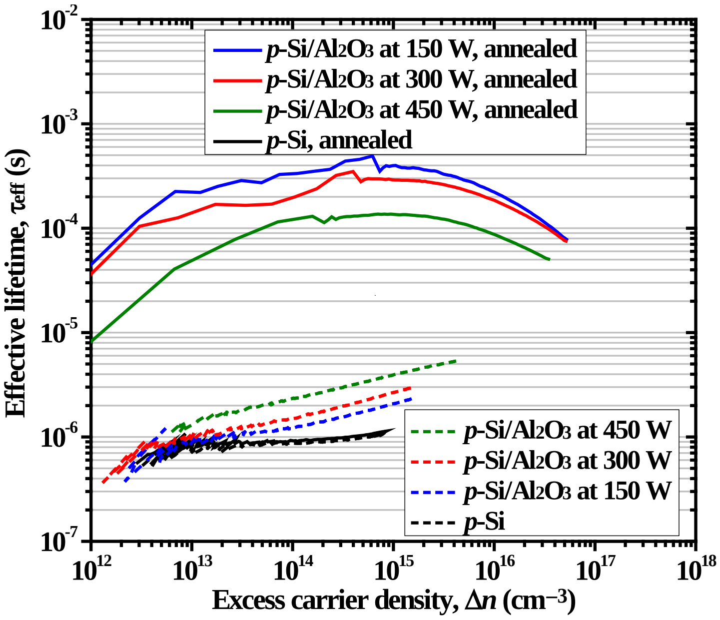

10^{-2}
10^{-3}
10^{-4}
10^{-5}
10^{-6}
10^{-7}
Effective lifetime, τ_{eff} (s)
10^{12}
10^{13}
10^{14}
10^{15}
10^{16}
10^{17}
10^{18}
Excess carrier density, Δn (cm^{-3})
p-Si/Al_2O_3 at 150 W, annealed
p-Si/Al_2O_3 at 300 W, annealed
p-Si/Al_2O_3 at 450 W, annealed
p-Si, annealed
p-Si/Al_2O_3 at 450 W
p-Si/Al_2O_3 at 300 W
p-Si/Al_2O_3 at 150 W
p-Si

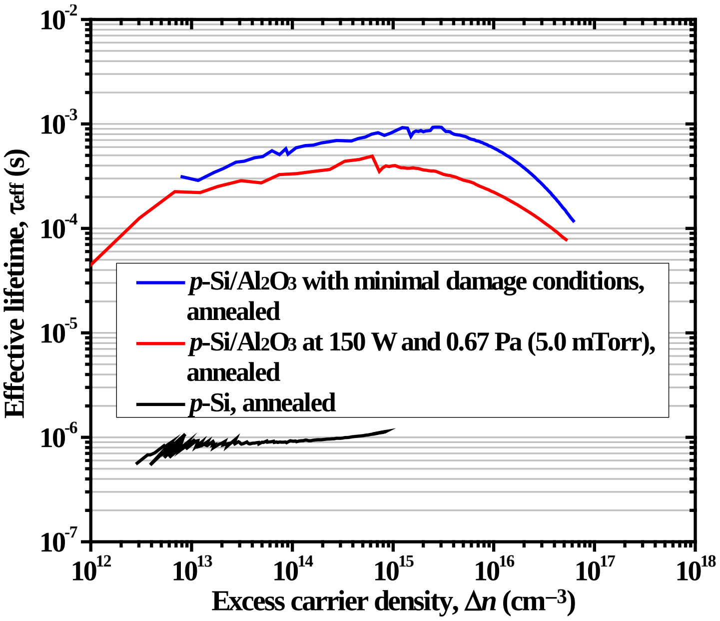
10^-2
10^-3
10^-4
10^-5
10^-6
10^-7
Effective lifetime, τeff (s)
p-Si/Al2O3 with minimal damage conditions, annealed
p-Si/Al2O3 at 150 W and 0.67 Pa (5.0 mTorr), annealed
p-Si, annealed
10^12
10^13
10^14
10^15
10^16
10^17
10^18
Excess carrier density, Δn (cm^−3)

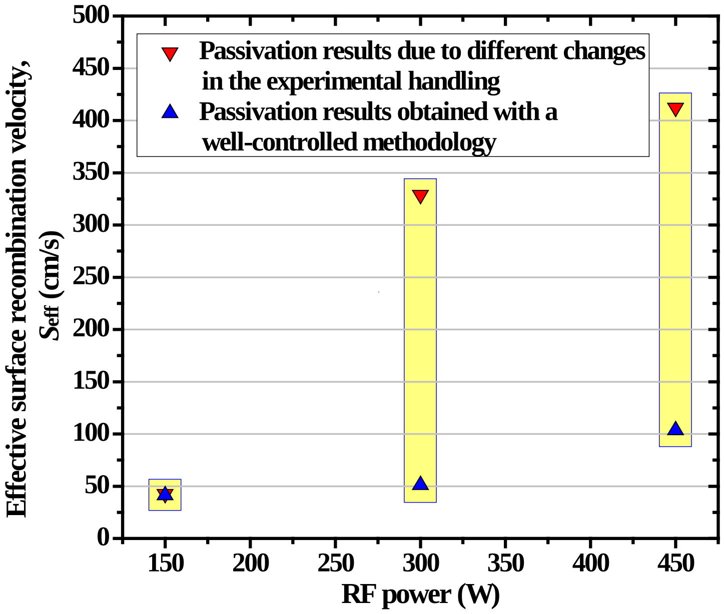
Effective surface recombination velocity,
S_{eff} (cm/s)
0
50
100
150
200
250
300
350
400
450
500
150
200
250
300
350
400
450
RF power (W)
▼ Passivation results due to different changes in the experimental handling
▲ Passivation results obtained with a well-controlled methodology